References

BRAUN, P. B., HORNSTRA, J. & LEENHOUTS, J. I. (1969). *Philips Res. Rep.* **24**, 85.
CROWTHER, R. A. & BLOW, D. M. (1967). *Acta Cryst.* **23**,544.
HORNSTRA, J. (1970). *Crystallographic Computing*, p. 103. Edited by F. R. AHMED. Copenhagen: Munksgaard.
HUBER, R. (1965). *Acta Cryst.* **19**, 353.
KENDREW, J. C. (1962). *Brookhaven Symp. Biol.* **15**, 216.
KOENIG, D. F. (1965). *Acta Cryst.* **18**, 663.
LATTMAN, E. E. & LOVE, W. E. (1970). *Acta Cryst.* B**26**, 1854.
NORDMAN, C. E. & NAKATSU, K. (1963). *J. Amer. Chem. Soc.* **85**, 353.
NORDMAN, C. E. & SCHILLING, J. W. (1970). *Crystallographic Computing*, p. 110. Edited by F. R. AHMED. Copenhagen: Munksgaard.
ROSSMANN, M. G. & BLOW, D. M. (1962). *Acta Cryst.* **15**, 24.
ROSSMANN, M. G., BLOW, D. M., HARDING, M. M. & COLLER, E. (1964). *Acta Cryst.* **17**, 338.
SCHILLING, J. W. (1970). *Crystallographic Computing*, p. 115. Edited by F. R. AHMED. Copenhagen: Munksgaard.
SPARKS, R. A. (1961). *Abstr. Amer. Cryst. Assoc. Meeting*, p. 37.
STEWART, J. M., KUNDELL, F. A. & BALDWIN, J. C. (1970). *The X-ray System of Crystallographic Programs*. Univ. of Maryland, College Park, Maryland.
TOLLIN, P. (1966). *Acta Cryst.* **21**, 613.
TOLLIN, P. (1969). *J. Mol. Biol.* **45**, 481.
TOLLIN, P. & COCHRAN, W. (1964). *Acta Cryst.* **17**, 1322.
WATSON, H. C. (1969). *Prog. Stereochem.* **4**, 299.
ZWICK, M. (1969). *Abstr. Amer. Cryst. Assoc. Winter Meeting*, p. 74.

Acta Cryst. (1972). A**28**, 143

Choice of Scans in X-ray Diffraction

BY S. A. WERNER

Scientific Research Staff, Ford Motor Company, Dearborn, Michigan, U.S.A. and Department of Nuclear Engineering, University of Michigan, Ann Arbor, Michigan, U.S.A.

(*Received* 20 *September* 1971)

In a recent paper (Werner, S. A. *Acta Cryst.* (1971). A**27**, 665) it was pointed out that the choice of scans in a neutron diffraction experiment should be based on the criterion that the diffracted beam enters the detector on its centerline for each angular setting of the crystal. The same criterion should be applied in X-ray diffraction. Since the spectral distribution of a source of X-rays and neutrons is quite different, conclusions regarding the optimum coupling between the detector and crystal motions are different in these two cases. In this paper, formulas are derived (within the framework of certain gaussian approximations) for the optimum scanning ratio g in equatorial plane X-ray diffraction experiments on single crystals. For the case when a monochromator is not used, g is independent of scattering angle $2\theta_B$ for a large range of instrumental parameters and Bragg angles θ_B. It is found that a θ–2θ scan is essentially never advisable. An expression for g is derived for the case when a planar monochromator is used in symmetric Bragg reflection. The optimum scan is found to depend on the scattering angle, but not in such a marked way as in the neutron case. Coupling the detector and crystal motions in the manner suggested allows one to decrease the acceptance aperture to its minimum width, thus keeping the background due to thermal diffuse scattering (TDS) and incoherent scattering as low as possible.

I. Introduction

The problem of the selection of scans in single crystal neutron diffraction experiments was discussed in a recent paper (Werner, 1971). The choice of scans in X-ray diffraction requires special attention because the geometry and spectral distribution of a source of X-rays and neutrons are quite different. Equatorial plane X-ray diffraction (like neutron diffraction) experiments on single crystals are generally carried out using either an ω-scan (crystal rotating, detector fixed) or a θ-2θ scan (detector coupled 2:1 to the crystal). In view of the widespread use of instrumentation involving tape-controlled and computer-controlled diffractometers, restricting the scanning of Bragg reflections to these two modes is not a necessary constraint. The purpose of this paper is to examine the question of whether there is in general a better way to scan Bragg reflections in X-ray diffraction.

Over the years a number of papers have been published on the theory of measuring integrated intensities and on the various geometrical considerations necessary in X-ray diffraction experiments on single crystals [see for example Alexander & Smith (1962), Burbank (1964), Ladell & Spielberg (1966)]. A summary of the results of these papers regarding the necessary size of the receiving aperture and the range of scan is given in the book by Arndt & Willis (1966). However, the analysis given in these papers does not permit the experimentalist to readily make a decision on the optimum coupling ratio between the detector and crystal motions. The intent of this paper is to derive an

expression for the optimum scanning ratio which can be easily used in practical experimental situations.

II. Filtered beam, point sample

In the neutron diffraction case, we used the obvious criterion in deriving the optimum scanning ratio g that *the diffracted beam should enter the detector on its centerline for all angular settings φ of the crystal.* That is, as the crystal is rotated by an angle $\Delta\varphi$, the detector should be moved by an angle $g\Delta\varphi$. A similar criterion should be applied in X-ray diffraction. There are several complications which make the X-ray problem more difficult; the most important of which is that the spectral distribution of incident X-rays is sharply peaked at the characteristic energies. We will treat the case here of filtered K-radiation (using a β filter or a set of balanced filters) and assume that the incident beam consists only of the $K\alpha_1$ and $K\alpha_2$ lines. That is, we assume the incident beam is described by two 'bell-shaped' distributions displaced from each other by a wave number δk. There is no angle–energy correlation in the incident beam. Thus, the beam incident on the sample is quite different in the X-ray and neutron cases. This difference naturally leads to quite different conclusions regarding the choice of scan.

A schematic diagram of a typical X-ray diffraction experiment is shown in Fig. 1. We first assume that the sample size is small in comparison to the X-ray focus. The angular distribution of X-rays incident on the sample is then due to the finite size of the X-ray focus. As the crystal is rotated through a Bragg reflection the angular distribution of reflected wave vectors will shift in a particular way dependent upon the nominal scattering angle $2\theta_B$, the sample mosaic spread η_s, the spectral distribution of the source, and the angular divergence of the incident beam. In order to obtain the integrated intensity, it is necessary for the detector to accept all of these Bragg scattered X-rays for each angular setting φ of the crystal with essentially equal efficiency. In order to reduce the background due to incoherent scattering and the correction necessary for thermal diffuse scattering, a slit is generally placed in front of the detector. This slit should be no wider than is necessary to accept all of the Bragg-scattered X-rays. For this to be the case, the detector must be moved as a function of the crystal angle φ. The necessary dimensions of the detector aperture have been discussed by several authors for the case of ω and θ–2θ scans [see for example Furnas (1957) or Burbank (1964)].

The intensity of the beam diffracted at an angle $2\theta_B+\gamma$, (where $2\theta_B$ is the nominal scattering angle) for a given setting φ of the crystal will involve an integration over wave number since the detector cannot distinguish between wave numbers k close to the nominal value k_0. That is

$$I(\gamma,\varphi)=\int J_0\left(\frac{\Delta k}{k_0},\gamma_0\right)R(\Delta_s)\mathrm{d}\left(\frac{\Delta k}{k_0}\right). \qquad (1)$$

J_0 is the distribution in wave number $\Delta k/k_0$ and angle γ_0 of the incident X-rays. $R(\Delta_s)$ is the reflectivity of the sample as a function of mosaic orientation angle Δ_s. Since the incident spectrum consists of two parts, $K\alpha_1$ and $K\alpha_2$, the diffracted beam consists of two parts, namely

$$I(\gamma,\varphi)=\int J_1\left(\frac{\Delta k}{k_0},\gamma_0\right)R(\Delta_s)\mathrm{d}\left(\frac{\Delta k}{k_0}\right)+\int J_2\left(\frac{\Delta k}{k_0},\gamma_0\right)R(\Delta_s)\mathrm{d}\left(\frac{\Delta k}{k_0}\right). \qquad (2)$$

The central wavenumber k_0 is generally taken to be $\frac{1}{3}k_2+\frac{2}{3}k_1$, where k_1 and k_2 are the wavenumbers corresponding to the centers of the $K\alpha_1$ and $K\alpha_2$ spectral lines [see Fig. 2(*a*)]. We have defined Δk to be the difference between any other wave number k and this arbitrary selection of the nominal k_0. The angular distribution of the incident beam is generally trapezoidal in shape with rounded edges as shown in Fig. 2(*b*). We will assume that the reflectivity of the crystal is gaussian, that is

$$R(\Delta_s)=p_s\exp\left(-\Delta_s^2/2\eta_s^2\right). \qquad (3)$$

The integrations indicated in equation (2) cannot be done analytically. Thus, in principle, a numerical integration is necessary for each Bragg reflection and for each set of instrumental parameters. This, of course, would be too cumbersome to be useful experimentally. However, if we approximate each of the spectral components, and the angular distribution of incident X-rays by gaussian functions, the integrations are straightforward. Since we are only interested in obtaining an expression for the optimum scanning ratio g and not the detailed nature of $I(\gamma,\varphi)$, these approximations will be found to be adequate. Thus, we suppose the incident beam is described by

$$J_0\left(\frac{\Delta k}{k_0},\gamma_0\right)=\{J_1\exp\left[-(k-k_1)^2/2k_0^2\xi_1^2\right]+J_2\exp\left[-(k-k_2)^2/2k_0^2\xi_2^2\right]\}\exp\left[-\frac{\gamma_0^2}{2\alpha_0^2}\right]. \qquad (4)$$

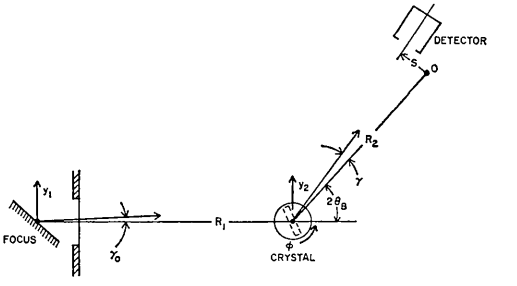

Fig. 1. A schematic diagram of a typical X-ray diffraction experiment. The distance between the X-ray focus and the crystal is R_1, and the distance between the detector and the crystal is R_2. The 'apparent' angle at which a given diffracted ray enters the detector is $\beta=s/R_2$, where the arc length s is measured from the nominal diffracted ray point O.

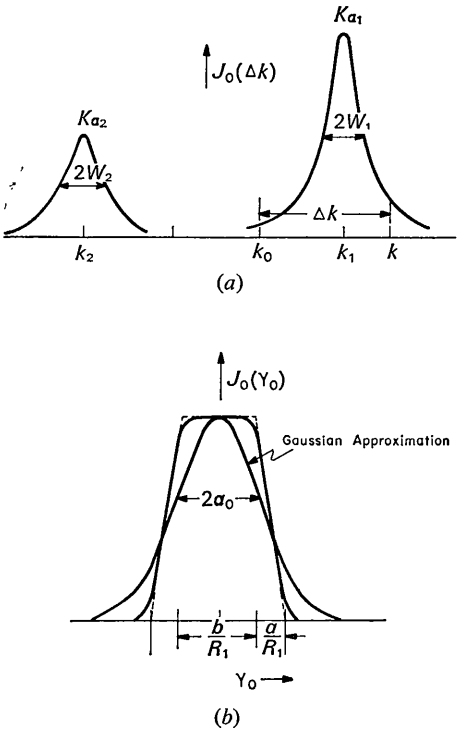

Fig. 2. (*a*). Assumed wave number distribution of the incident beam. (*b*) Diagram showing the assumed gaussian approximation to a trapezoidal angular distribution of the incident beam impinging upon a point sample.

The parameters ξ_1, ξ_2 and α_0 are chosen such that the area and height of the gaussian functions are the same as for the Cauchy and trapezoidal functions, namely,

$$\xi_i=\sqrt{(\pi/2)}w_i \tag{5a}$$

$$\alpha_0=\frac{2a+b}{\sqrt{(2\pi)}R_1}. \tag{5b}$$

w_i is the half-width at half-maximum of the spectral line $K\alpha_1$ or $K\alpha_2$. a and b are horizontal dimensions associated with the X-ray focus. R_1 is the distance between the source and the sample (see Figs. 1 and 2).

In order to perform the integrations indicated in equation (2) we must express γ_0 and Δ_s in terms of γ, φ and $\Delta k/k_0$. This is easily done; the results are

$$\gamma_0=\gamma-2\frac{\Delta k}{k_0}\varepsilon\tan\theta_B \tag{6a}$$

and

$$\Delta_s=\gamma-\varphi-\frac{\Delta k}{k_0}\varepsilon\tan\theta_B. \tag{6b}$$

All angles are defined to be positive for rotations in the counter-clockwise sense, and ε gives the sense of scattering (not important in this problem). Inserting these relations into equation (2), we find that the intensity for a given diffracted-ray direction γ and crystal setting $\varphi(=\theta-\theta_B)$ is

$$I(\gamma,\varphi)=I_1\exp\{-[\gamma-\Gamma_1(\varphi)-2\varphi_1]^2/2\delta_1^2-(\varphi-\varphi_1)^2/2\sigma_1^2\}$$
$$+I_2\exp\{-[\gamma-\Gamma_2(\varphi)-2\varphi_2]^2/2\delta_2^2-(\varphi-\varphi_2)^2/2\sigma_2^2\}. \tag{7}$$

The width of the rocking curve associated with each spectral component ($K\alpha_1$, $K\alpha_2$) is given by σ_i. The width of each component of the outgoing diffracted beam δ_i is independent of the crystal setting. Expressions for σ_i and δ_i are given in Appendix *A*.

The centroid of the diffracted rays for each spectral component is shifted by an angle $2\varphi_i$ (relative to the nominal scattering angle $2\theta_B$) due to the selection of k_0 to lie between the $K\alpha_1$ and $K\alpha_2$ lines. This angle increases with increasing scattering angle according to

$$\varphi_i=-\tan\theta_B\left(\frac{k_i-k_0}{k_0}\right). \tag{8}$$

There is an additional shift Γ_i of the diffracted rays which is a linear function of the crystal setting, namely

$$\Gamma_i(\varphi)=g_i(\varphi-\varphi_i), \tag{9}$$

where the dependence of g_i on the instrumental parameters is found to be

$$g_i=\frac{\alpha_0^2+2\tan^2\theta_B\xi_i^2}{\eta_s^2+\tan^2\theta_B\xi_i^2+\alpha_0^2}. \tag{10}$$

This is a rather simple formula; however, the implications of it are rather surprising. The physical importance is the following: if the diffractometer is aligned on a given Bragg reflection such that the nominal incident wave vector $\mathbf{k}_0$ is reflected into the center of the detector when the crystal is set at $\varphi=0$, the centroids of the diffracted rays associated with the $K\alpha_1$ and $K\alpha_2$ lines will be displaced to the left and to the right

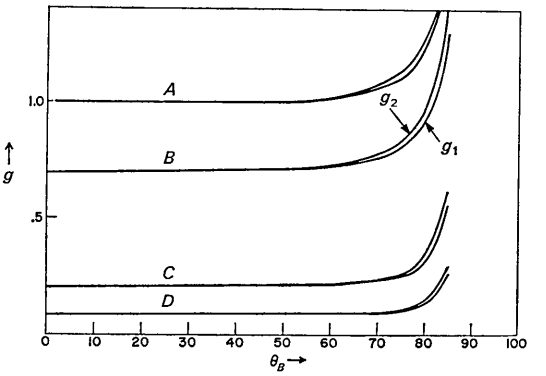

Fig. 3. Curves showing the variation of the optimum scanning ratio g as a function of Bragg angle. The spectral width parameters were taken as $\xi_1=2{\cdot}57\times10^{-4}$, $\xi_2=2{\cdot}82\times10^{-4}$ [appropriate to Mo radiation according to equation (5*a*)]. The collimation parameter was chosen to be $\alpha_0=0{\cdot}15°$. Curve (*A*) is drawn for a mosaic spread $\eta_s=0{\cdot}01°$, (*B*) for $\eta_s=0{\cdot}1°$, (*C*) for $\eta_s=0{\cdot}3°$ and (*D*) for $\eta_s=0{\cdot}5°$.

respectively of the center of the detector aperture. As the crystal is rotated by an angle φ, the diffracted $K\alpha_1$ component will shift by an angle $g_1\varphi$ and the $K\alpha_2$ component will shift by $g_2\varphi$. Thus, in order to maintain the original alignment of the diffracted rays with respect to the center of the detector aperture, the detector should be rotated by the angle $g_1\varphi$ for $K\alpha_1$ and $g_2\varphi$ for $K\alpha_2$. This, of course, cannot be done. However, g_1 and g_2 differ only because the widths of the $K\alpha_1$ and $K\alpha_2$ lines are slightly different. This difference is only 10% for Mo radiation [see Compton & Allison (1935) p. 745]. In addition the spectral widths ξ_i are quite often very small in comparison with the collimation α_0 and the sample mosaic spread η_s. In this case

$$g_1=g_2=\frac{\alpha_0^2}{\eta_s^2+\alpha_0^2}. \tag{11}$$

Plots of g_i using widths appropriate to Mo radiation and for $\alpha_0=0{\cdot}15°$ for various mosaic spreads η_s are shown in Fig. 3. It is seen that the difference between g_1 and g_2 only shows up at very large scattering angle. Thus, to a very good approximation, a scanning ratio which is the average of g_1 and g_2 is optimum. That is, the coupling between the detector and crystal motions should be

$$g=\frac{g_1+g_2}{2}. \tag{12}$$

This choice of scan will keep the diffracted beam aligned with the detector. *It will be noted that a θ–2θ scan is essentially never advisable.* In fact, in the simplest case to consider, namely that of a perfect crystal ($\eta_s=0$) and a monoenergetic source ($\xi_i=0$), the coupling between the detector and the crystal should be 1:1 not 2:1!

In order to emphasize the seriousness of not performing the optimum scan, we have plotted in Fig. 4(*a*) the angular distribution of the diffracted beam as given by equation (7) for a given set of parameters ($\eta_s=0{\cdot}1°$, $\alpha_0=0{\cdot}15°$, $\theta_B=20°$) using Mo radiation. We have assumed that the relative intensity of $K\alpha_1$ and $K\alpha_2$ is 2:1. For an ω scan, the center of the detector remains at $\gamma=0$. Thus, as the crystal is rotated from negative to positive φ, the diffracted beam moves across the detector apertures from left to right. The same distri-

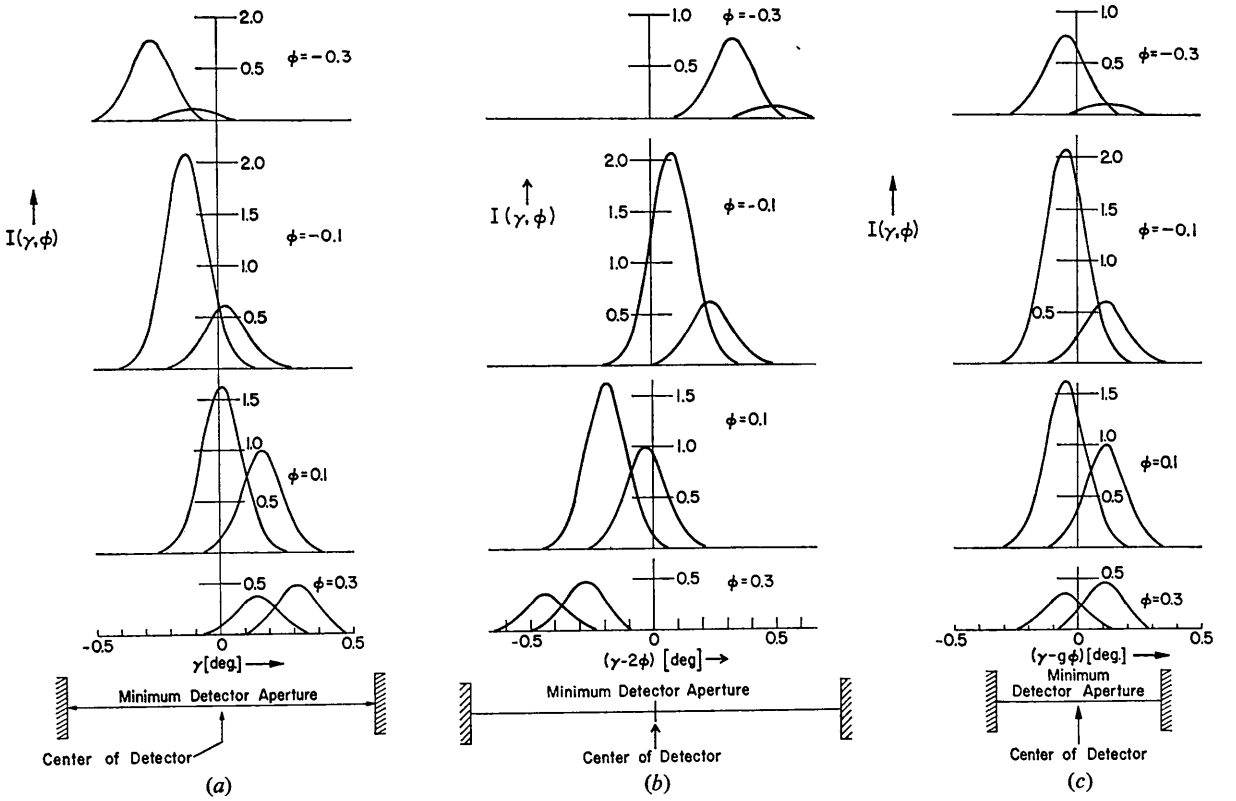

Fig. 4. This figure shows the diffracted beam distribution [as given by equation (7)] plotted with an abscissa appropriate to (*a*) an ω scan, (*b*) a θ–2θ scan, (*c*) an optimum scan. The collimation parameter $\alpha_0=0{\cdot}15°$, the mosaic spread $\eta_s=0{\cdot}1°$, the Bragg angle $\theta_B=20°$. The separation between the $K\alpha_1$ and $K\alpha_2$ lines was taken as $(k_1-k_2)/k_0=5{\cdot}9\times10^{-3}$, appropriate to Mo radiation, and the relative intensity of the two lines was assumed to be 2:1. It is noted that the detector aperture (as shown schematically here) can be considerably narrower if the optimum scan is performed than for an ω-scan or a θ–2θ scan. The slit widths shown are not precise (a matter of judgement) and are only shown to illustrate the possibility of using a narrower receiving aperture.

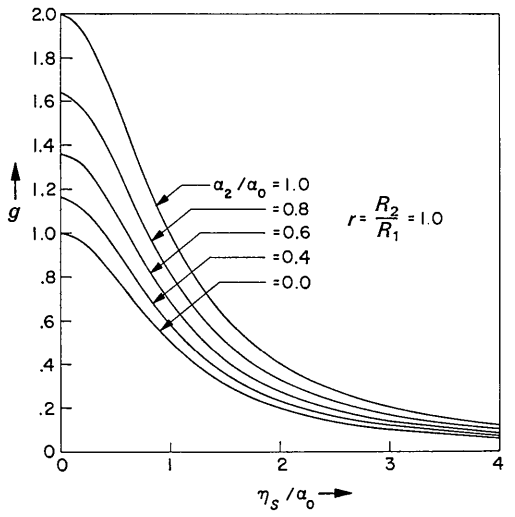

Fig. 5. Dependence of the optimum scanning ratio g on the ratio of the mosaic spread η_s to the net collimation parameter α_0. These curves are drawn for various α_2/α_0, where this ratio gives the fraction of the collimation which is due to the crystal size. The relative distance between the detector and the crystal (R_2) and the distance between the source and the crystal (R_1) is $r=1{\cdot}0$.

butions are plotted in Fig. 4(*b*) with $\gamma-2\varphi$ as the abscissa, which is appropriate for a θ–2θ scan. The center of the detector is at $\gamma-2\varphi=0$. Thus, we see that in this case the diffracted beam moves from right to left across the detector as the crystal is rotated from negative to positive φ. That is, the detector is moving too rapidly in order to keep the diffracted beam aligned with its centerline. In Fig. 4(*c*), the same distribution is plotted with $\gamma-g\varphi$ as the abscissa. In this case the optimum scanning ratio g is 0·694, and we note that this coupling ratio maintains the alignment of the detector with the diffracted beam. An important benefit of coupling the detector and the crystal together in the way suggested here is that the size of the detector aperture may be reduced to its minimum size, thus reducing the background due to TDS and incoherent scattering.

III. Effect of crystal size

In § II we assumed that the crystal size was small in comparison to the size of the X-ray focus. The fact that in some cases the crystal may be of comparable size is important. Not only is the cross-fire, say α_0, of the incident beam increased, but the center of gravity of the diffracted beam within the crystal shifts as the crystal is rotated. That is, the 'X-ray center' of the crystal does not coincide with its geometric center and is dependent upon crystal angle φ. Thus the detector should be moved as a function of φ in order to remain aligned with the diffracted beam. In fact, the detector should really be *translated* as a function of φ. However since the crystal size is generally small in comparison with the distance R_2 between the detector and the crystal, this necessary translation can be taken care of by an additional rotation of the detector. A precise calculation of this effect will of course depend on the size and shape of the crystal. Since we are only interested in obtaining an expression for the optimum scanning ratio we will make certain approximations so that the problem is analytically tractable.

In this case we are interested in calculating the net diffracted X-ray intensity entering the detector aperture at a distance s away from the nominal ray on an arc of radius R_2 (see Fig. 1) for each setting of the crystal φ. That is, we are interested in the intensity $I(s,\varphi)$ or equivalently $I(\beta,\varphi)$ where $\beta=s/R_2$. This involves integrating the diffracted intensity over wave number and over all of the possible ray directions γ leading from the crystal to the point s on the detector aperture.

We write the incident intensity J_0 as a function of wave number $\Delta k/k_0$ and the position y_1 (measured perpendicular to the incident beam direction) on the X-ray focus. The reflectivity R of the crystal is now a function of both the mosaic orientation angle Δ_s and the position in the crystal from which the diffracted beam originates. We make the following approximations:

Approximation (1). The trapezoidal shape of the y_1 dependence of the incident beam is replaced by a gaussian (as in § II), namely

$$J_0(y_1)\sim\exp(-y_1^2/2\omega_1^2)\,. \tag{13}$$

Approximation (2). The crystal shape is approximated by a thin disk with the plane of the disk containing the scattering vector (see Fig. 1), and the reflectivity drops off from the center of the crystal as a gaussian

$$R\sim\exp(-y_2^2/2\omega_2^2)\,. \tag{14}$$

Thus, the diffracted intensity as a function of the 'apparent' outgoing angle β and crystal setting φ is

$$I(\beta,\varphi)=\int J_0\left(\frac{\Delta k}{k_0},\,y_1\right)R(\Delta_s,y_2)\mathrm{d}\gamma\mathrm{d}\left(\frac{\Delta k}{k_0}\right). \tag{15}$$

At first sight approximation (2) might appear to be excessively severe. However, it is clear that we have retained the essential physical ingredients of the problem, and the accuracy to which our result for the optimum scanning ratio g approximates the result of a detailed numerical integration for a given crystal shape will depend on how we choose the equivalent gaussian parameter ω_2. We suggest that this should be done in the same way as in § II; namely, the gaussian function approximating the y_2 dependence of the reflectivity should have the same area and height as the more exact expression.

For example, for a 'transparent' sphere of radius ϱ the reflectivity falls off quadratically with y_2 as

$$R(y_2)=1-(y_2/\varrho)^2\,, \tag{16}$$

so that we would take

$$\omega_2=\tfrac{4}{3}\frac{1}{\sqrt{(2\pi)}}\varrho\,. \tag{17}$$

In §II we found that the selection of the position of the nominal wavevector k_0 to lie between $K\alpha_1$ and $K\alpha_2$ simply displaces the mean diffracted-ray direction by $2\varphi_i$ and the maximum of crystal rocking curve by φ_i. Consequently, we will let k_0 coincide with the center of the $K\alpha_1$ line (or the $K\alpha_2$ line) in order to simplify the algebra and suppose that the incident beam consists of only one line of the doublet. The result [equation (20)] can then be modified to include both lines by making the substitutions $\beta \rightarrow \beta - 2\varphi_i$ and $\varphi \rightarrow \varphi - \varphi_i$.

In order to perform the integration indicated in equation (15) we must express y_1, y_2, and Δ_s in terms of β, φ, γ, and $\Delta k/k_0$. This is easily done from the geometry of Fig. 1 and the results are

$$y_1 = -(R_1+R_2)\gamma + 2\varepsilon \tan\theta_B R_1 \frac{\Delta k}{k_0} + R_2\beta\,, \qquad (18)$$

and

$$y_2 = R_2\beta - R_2\gamma\,. \qquad (19)$$

Δ_s is given by equation (6*b*). With these substitutions the intensity as a function of the 'apparent' diffracted-ray direction β and crystal setting φ is found to be of the form

$$I(\beta,\varphi) = I_0 \exp\{-[\beta - \Gamma(\varphi)]^2/2\delta^2 - \varphi^2/2\sigma^2\}\,. \qquad (20)$$

The center of the diffracted beam again shifts linearly with the crystal setting according to

$$\Gamma(\varphi) = g\varphi\,. \qquad (21)$$

The general expressions for σ, δ and g are given in Appendix B. When the width of the spectral line is narrow in comparison with the collimation and mosaic spread, the optimum scanning ratio is

$$g = \frac{(r+r^2)\alpha_2^2 + \alpha_1^2}{r^2\alpha_2^2 + \alpha_1^2 + \eta_s^2}\,. \qquad (22)$$

where r is the ratio of the distance between the detector and the sample (R_2) to the distance from the source to the sample (R_1). The collimation parameters (α_1, α_2) associated with the size of the source and the sample are $\alpha_1 = \omega_1/R_1$ and $\alpha_2 = \omega_2/R_1$ respectively. If one were only to take into account the angular variables and were to ignore the effect of the shift of the 'X-ray' center of the crystal with φ this expression would reduce to equation (11), where the net collimation parameter is

$$\alpha_0 = \sqrt{\alpha_1^2 + \alpha_2^2}\,. \qquad (23)$$

In Fig. 5 we have plotted the optimum scanning ratio g given by equation (22) as a function of the ratio of the mosaic spread η_s to the net collimation parameter α_0 (for the case $r = 1{\cdot}0$). The ratio α_2/α_0 gives the fraction of the net collimation which is due to the finite size of the crystal. It is noted that the only case when a θ–2θ scan is optimum is for a perfect crystal ($\eta_s = 0$) and a point source ($\alpha_2/\alpha_0 = 1{\cdot}0$). The translational effect of the X-ray center of the crystal on g is important when the size of the crystal is comparable to the projected size of the focus. It generally requires that the detector should be moved more rapidly with respect to the crystal than would be the case if this translational effect were absent.

For a wide range of scattering angles and experimental parameters, the expression for the optimum scanning ratio g given in equation (22) will be adequate. Although the general expression for g given in Appendix *B* is rather complicated, for a given experiment with a definite set of parameters, it is simply a single curve as a function of Bragg angle similar to those drawn in Fig. 3.

An obvious effect which is not given by the analysis outlined here is illustrated in Fig. 6. Suppose the source is monoenergetic and small in comparison to the sample. Then, as the sample is rotated from negative angles to positive angles, the diffracting region of the crystal shifts from one edge of the crystal [Fig. 6(*a*)] through the middle [Fig. 6(*b*)] to the other edge [Fig. 6(*c*)]. Thus, the diffracted beam is first spatially narrow, goes through a maximum in width at $\varphi = 0$ and then narrows again as the crystal is rotated. Since we have approximated the crystal shape by a thin disk (Approximation 2), this effect due to the finite thickness of the crystal is not included, and the result obtained for the width of the diffracted beam δ is independent of φ. As we have pointed out, this approximation is not serious in the calculation of the optimum scanning ratio. However, in calculating the width of the receiving aperture, it should be taken into account if the sample is large. It is apparent that a derivation of the change in the width of the diffracted beam as a function of φ due to this effect could be made. Since

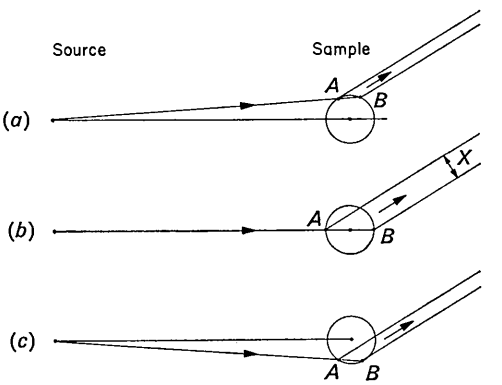

Fig. 6. Diagram illustrating the effect of the finite thickness of the sample on the width of the diffracted beam. For a perfect crystal ($\eta_s = 0$) and a point source which is monoenergetic, the diffracted beam originates on one side of the crystal on the plane between *A* and *B* for negative crystal settings φ and is spatially narrow (*a*). As the crystal is rotated through the peak of the Bragg reflection the beam broadens (*b*) and then narrows again (*c*).

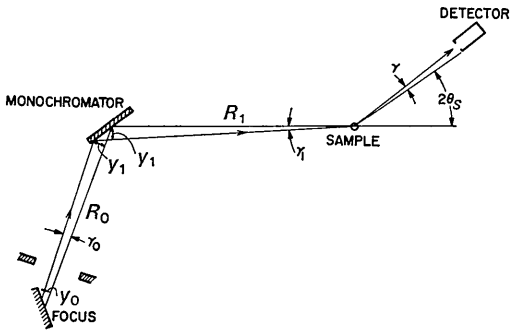

Fig. 7. Schematic diagram of an X-ray diffraction experiment in which a planar monochromator is used in symmetric Bragg reflection.

it is not likely that one will want to change the detector slit width progressively during a scan, a calculation of this kind would not be very useful. Simply adding a width due to this effect will give an acceptable prescription for calculating the necessary detector aperture for an optimum scan. The maximum projected width X [see Fig. 6(*b*)] should be used.

IV. Monochromated source

There are numerous geometries which should be considered in deriving an expression for the optimum scanning ratio g when a monochromating crystal is used. We treat only the simplest case here; that is, a planar monochromator used in symmetric Bragg reflection and a point sample as shown in Fig. 7. Generalizing this calculation to bent crystal monochromators, asymmetrically cut monochromators, and samples of finite size is not a difficult task.

We are again interested in obtaining an expression for the diffracted intensity as a function of the crystal angle φ and the outgoing ray angle γ. The nominal wave vector $\mathbf{k}_0$ will be chosen to coincide with one of the spectral components say $K\alpha_1$. In this case, this selection is not arbitrary since the orientation of the monochromator determines the nominal wavelength. Thus, the diffracted beam intensity due to $K\alpha_1$ is

$$I(\gamma,\varphi)=\int J_0\left(\frac{\Delta k}{k_0},\, y_0\right)R_m(\Delta_m)R_s(\Delta_s)\,\mathrm{d}\left(\frac{\Delta k}{k_0}\right). \quad (24)$$

The spectral ($\Delta k/k_0$) and spatial (y_0) distribution of the source of X-rays is approximated by gaussian function as was done in §§ II and III. That is we take

$$J_0(\Delta k/k_0, y_0)=J_0\exp\left[-(\Delta k)^2/2k_0^2\xi^2-y_0^2/2\omega_0^2\right]. \quad (25)$$

R_m and R_s are the reflectivities of the monochromator and sample. Δ_m and Δ_s are the mosaic orientation angles. In order to perform the integration in equation (24) it is necessary to express y_0, Δ_m and Δ_s in terms of γ, φ and $\Delta k/k_0$. This can easily be done from the geometry of Fig. 7. The results are

$$y_0=\gamma[R_1-R_0]+\frac{\Delta k}{k_0}[2R_0(M+2S)-2R_1S] \quad (26a)$$

$$\Delta_m=\gamma-(M+2S)\frac{\Delta k}{k_0} \quad (26b)$$

and

$$\Delta_s=\gamma-\varphi-S\frac{\Delta k}{k_0}. \quad (26c)$$

Where

$$M=\varepsilon_m\tan\theta_m, \quad (27a)$$

and

$$S=\varepsilon_s\tan\theta_s. \quad (27b)$$

ε_m and ε_s give the sense of scattering at the monochromator and the sample respectively, and are ± 1 depending upon whether the scattering is to the left or to the right.

Using these results, the integration over wave number gives a gaussian function for the diffracted beam intensity, namely

$$I(\gamma,\varphi)=I_0\exp\left[-(\gamma-g\varphi)^2/2\delta^2-\varphi^2/2\sigma^2\right]. \quad (28)$$

Expressions for the width parameters σ and δ are given in Appendix *C*. In order to keep the centroid of the diffracted beam aligned with the centerline of the detector we must move the detector by the angle $g\varphi$ when the crystal is rotated through the angle φ. We find that g is given by the expression

$$g=\frac{\dfrac{1}{\eta_s^2}\left[\dfrac{1}{\xi^2}+\left(\dfrac{2(M+2S)}{\alpha_0}-\dfrac{2S}{\alpha_1}\right)\left(\dfrac{2M+3S}{\alpha_0}-\dfrac{S}{\alpha_1}\right)\right]}{\dfrac{1}{\xi^2}\left[\left(\dfrac{1}{\alpha_1^2}-\dfrac{1}{\alpha_0^2}\right)+\dfrac{1}{\eta_m^2}+\dfrac{1}{\eta_s^2}\right]+\dfrac{1}{\eta_m^2}\left[\dfrac{M+2S}{\alpha_1}+\dfrac{1-2S}{\alpha_1}\right]^2+\dfrac{1}{\eta_s^2}\left[\dfrac{2M+3S}{\alpha_0}-\dfrac{S}{\alpha_1}\right]^2-\dfrac{(S+M)^2}{\eta_s^2\eta_m^2}}. \quad (29)$$

η_m and η_s are the mosaic spread parameters of the monochromator and sample respectively. $\alpha_0(=\omega_0/R_0)$, and $\alpha_1(=\omega_0/R_1)$ are the collimation parameters.

The wide variation of this expression for the optimum scanning ratio g is shown in Fig. 8. These diagrams are drawn for a particular selection of parameters: $\theta_m=30°$, $\alpha_0=0{\cdot}1°$, $\alpha_1=0{\cdot}2°$, $\xi=0{\cdot}0147°$. When the monochromator mosaic spread is small, the optimum scanning ratio exhibits a gentle maximum near the parallel position ($\varepsilon_s\theta_s=-30°$). As the sample mosaic spread increases, the optimum scan approaches an ω-scan. For a large mosaic monochromator, g is consistently less than 1 and again approaches 0 as the sample mosaic spread is increased.

V. Conclusions

The central theme of this paper is that the crystal and detector motions should be coupled in a manner which keeps the centroid of the diffracted beam aligned with the centerline of the detector. This obviously allows one to use the minimum possible detector aperture, thus keeping the background due to thermal diffuse and incoherent scattering as low as possible. Performing experiments in this manner should prove to be particularly important for high index reflections where the Bragg peaks are weak due to the small form factor and the large Debye–Waller factor ($2W$), and the TDS background is large.

Although some of the expressions we have derived for the optimum scanning ratio g may appear to be rather complicated, for a given experiment g is a single valued function of the Bragg angle θ_s. Implementing the use of the optimum scanning ratio for tape controlled and computer controlled diffractometers is straightforward and adds essentially no complication to the accumulation of data. In certain cases the expression for g reduces to a very simple formula, for example equation (11). Whether or not the approximations which we have used need further refinement will await experimental confirmation.

APPENDIX *A*

Expression for σ_i and δ_i for the case of a point sample

The width of the rocking curve σ_i associated with each spectral component is given by

$$\sigma_i^2 = \eta_s^2 + \tan^2\theta_B\xi_i^2 + \alpha_0^2 . \qquad (A1)$$

The angular width of the diffracted beam δ_i is found to be

$$\delta_i^2 = \frac{\alpha_0^2\eta_s^2 + 4\tan^2\theta_B\eta_s^2\xi_i^2 + \tan^2\theta_B\alpha_0^2\xi_i^2}{\eta_s^2 + \tan^2\theta_B\xi_i^2 + \alpha_0^2} . \qquad (A2)$$

APPENDIX *B*

Expression for σ, δ, g for the case of a finite sample

For the range of scattering angles $2\theta_B$, and the parameters η_s, α_1 and α_2 for which the spectral width cannot be ignored, the optimum scanning ratio is

$$g = -N_2/2N_1 , \qquad (B1)$$

and the width parameters σ and δ are found from the expressions

$$\frac{1}{\sigma^2} = N_3 - N_2^2/4N_1 \qquad (B2)$$

and

$$\delta^2 = 1/N_1 . \qquad (B3)$$

N_1, N_2 and N_3 depend on the instrumental parameters and the Bragg angle θ_B;

$$N_1 = \left[\frac{r^2}{A_1\xi^2\alpha_1^2} + \frac{1}{\alpha_2^2} + \frac{\tan^2\theta_B r^2}{A_1\alpha_1^2\eta_s^2}\right] - \left[\frac{2\tan^2\theta_B(r-r^2)}{\eta_s^2\alpha_1^2A_1} - \frac{2(r+r^2)}{\xi^2\alpha_1^2A_1} - \frac{2}{\alpha_2^2}\right]^2 \Big/ 4A_2 . \qquad (B4)$$

$$N_2 = \frac{-4\tan^2\theta_B r}{\alpha_1^2\eta_s^2A_1} + 2\left[\frac{\tan^2\theta_B(r-r^2)}{\eta_s^2\alpha_1^2A_1} - \frac{(r+r^2)}{\xi^2\alpha_1^2A_1} - \frac{1}{\alpha_2^2}\right] \times \left[\frac{1}{\xi^2\eta_s^2A_1} + \frac{2\tan^2\theta_B(1-r)}{\eta_s^2\alpha_1^2A_1}\right] \Big/ A_2 . \qquad (B5)$$

$$N_3 = \left[\frac{1}{\eta_s^2\xi^2A_1} + \frac{4\tan^2\theta_B}{\alpha_1^2\eta_s^2A_1}\right]^2 - \left[\frac{1}{\xi^2\eta_s^2A_1} + \frac{2\tan^2\theta_B(1-r)}{\eta_s^2\alpha_1^2A_1}\right]^2 \Big/ A_2 . \qquad (B6)$$

Where

$$A_1 = \frac{1}{\xi^2} + \frac{4\tan^2\theta_B}{\alpha_1^2} + \frac{\tan^2\theta_B}{\eta_s^2} . \qquad (B7)$$

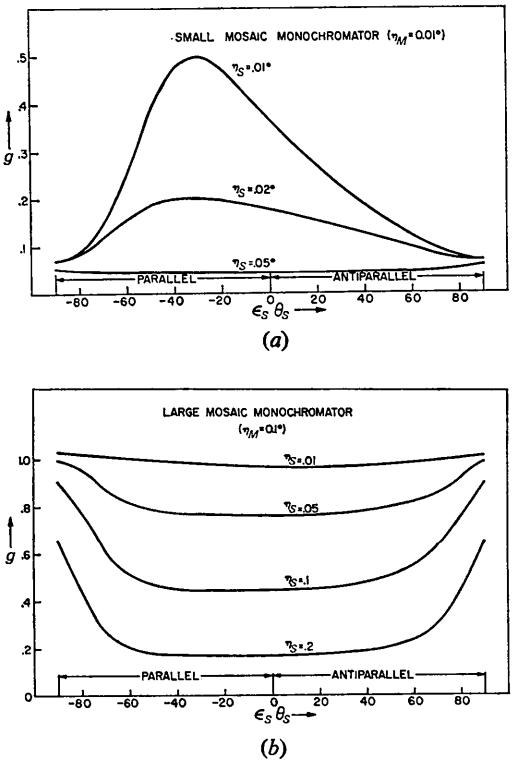

Fig. 8. (*a*) Optimum scanning ratio g as a function of the sample Bragg angle θ_s for a narrow mosaic monochromator. The monochromator Bragg angle θ_m was taken to be 30°, and the collimation parameters $\alpha_0 = 0{\cdot}1°$ and $\alpha_1 = 0{\cdot}2°$. The gaussian approximated spectral width parameter $\xi = 0{\cdot}0147°$. (*b*) Same parameters as in (*a*), but for a large mosaic monochromator.

and

$$A_2=\frac{(1+r)^2\eta_s^2+\alpha_1^2+\xi^2\tan^2\theta_B(1-r)^2}{\eta_s^2\alpha_1^2+4\tan^2\theta_B\xi^2\eta_s^2+\tan^2\theta_B\xi^2\alpha_1^2}+\frac{1}{\alpha_2^2}. \quad (B8)$$

APPENDIX C
Monochromated source, expressions for σ and δ

The width parameter δ of the diffracted beam is given by

$$\delta^2=4A\Big/\left[4A\left(\frac{a^2}{\omega_0^2}+\frac{1}{\eta_m^2}+\frac{1}{\eta_s^2}\right)-\left(\frac{2ab}{\omega_0^2}-\frac{2(M+2S)}{\eta_m^2}-\frac{2S}{\eta_s^2}\right)^2\right]. \quad (C1)$$

The rocking curve width parameter σ is found from the expression

$$\frac{1}{\sigma^2}=\frac{(A-S^2)}{\eta_s^2A}-\frac{g^2}{\delta^2}. \quad (C2)$$

Where

$$A=\frac{1}{\xi^2}+\frac{b^2}{\omega_0^2}+\frac{(M+2S)^2}{\eta_m^2}+\frac{S^2}{\eta_s^2}. \quad (C3)$$

$$a=R_1-R_0, \quad (C4)$$

and,

$$b=2(M+2S)R_0-2SR_1. \quad (C5)$$

References

ALEXANDER, L. E. & SMITH, G. S. (1962). *Acta Cryst.* **15**, 983.

ARNDT, U. W. & WILLIS, B. T. M. (1966). *Single Crystal Diffractometry*, p. 265. Cambridge University Press.

BURBANK, R. D. (1964). *Acta Cryst.* **17**, 434.

COMPTON, A. H. & ALLISON, S. K. (1935). *X-rays in Theory and Experiment*, p. 745. New York: Van Nostrand

FURNAS, T. C. (1957). '*Single Crystal Orienter Instruction Manual*', General Electric Company.

LADELL, J. & SPIELBERG, N. (1966). *Acta Cryst.* **21**, 103.

WERNER, S. A. (1971). *Acta Cryst.* **27**, 665.

Acta Cryst. (1972). A**28**, 151

Modified Ewald Construction for Neutrons Reflected by Moving Lattices

BY B. BURAS

Department of Physics, H. C. Ørsted Institute, University of Copenhagen, and the Danish Atomic Energy Commission Research Establishment, Risø, Denmark

AND T. GIEBULTOWICZ

Institute of Experimental Physics, University of Warsaw, Poland

(*Received* 4 *October* 1971)

A simple reciprocal lattice construction is presented which, in the case of neutrons reflected by moving lattices, permits Ewald construction directly in the laboratory frame without transforming the neutron velocity from the laboratory frame to the moving-crystal frame and back. Some special features and cases of the reflexion process – as seen in the laboratory frame – are discussed.

In recent years, an increased interest in neutron scattering by moving lattices has been shown (Lowde, 1957; Brockhouse, 1961; Shull & Gingrich, 1964; Meister, 1967; Shull, Morash & Rogers, 1968; Buras, Giebultowicz, Minor & Rajca, 1970). The experiments performed so far have shown easily measured changes in the reflexion process due to some kind of Doppler effect. It also seems plausible that the neutron diffraction effects observed in vibrating piezoelectric crystals by Galociova, Tichy, Zelenka, Michalec & Chalupa (1970) are strongly influenced by the Doppler effect (Buras, Giebultowicz, Minor & Rajca, to be published).

As proposed by Lowde (1957), and followed by Brockhouse (1961), Shull & Gingrich (1964), and Shull *et al.* (1968), the process of neutron diffraction by moving lattices is usually depicted in the reciprocal lattice space (Fig. 1) and consists of three steps: (1) the incident neutron velocity, $\mathbf{v}_i$, is transformed from the laboratory space to the moving-crystal space where it is equal to $\mathbf{u}_i$, (2) the reflected neutron velocity, $\mathbf{u}_r$, in the moving-crystal frame is found by means of Ewald construction, and (3) the reflected neutron velocity, $\mathbf{u}_r$, is transformed from the crystal moving frame to the laboratory frame, and the reflected neutron velocity, $\mathbf{v}_r=\overrightarrow{\mathrm{DE}}$, in the laboratory frame is finally obtained. This paper presents a simple procedure which directly permits reciprocal-lattice construction in the laboratory frame without laborious transformation from